HHS Public Access

Author manuscript

Ann Thorac Surg. Author manuscript; available in PMC 2023 February 01.

Published in final edited form as:

Ann Thorac Surg. 2022 February ; 113(2): 654–662. doi:10.1016/j.athoracsur.2020.12.013.

Dynamic Annular Modeling of the Unrepaired Complete Atrioventricular Canal Annulus

Hannah H. Nam, BA[1], **Patrick V. Dinh, BA**[1], **Andras Lasso, PhD**[2], **Christian Herz, MS**[1], **Jing Huang, PhD**[3], **Adriana Posada, MD**[1], **Ahmed H Aly, PhD**[4], **Alison M. Pouch, PhD**[5], **Saleha Kabir, MD**[6], **John Simpson, MD**[6], **Andrew C. Glatz, MD, MSCE**[7], **David M. Harrild, MD, PhD**[8], **Gerald Marx, MD**[8], **Gabor Fichtinger Dr. Univ.**[2], **Meryl S. Cohen, MD**[7], **Matthew A. Jolley, MD**[1,7]

[1]Department of Anesthesiology and Critical Care Medicine, Children's Hospital of Philadelphia, Philadelphia, PA

[2]Laboratory for Percutaneous Surgery, Queen's University, Kingston, ON

[3]Department of Biostatistics, Epidemiology and Informatics, University of Pennsylvania; and Department of Pediatrics, Children's Hospital of Philadelphia, Philadelphia, PA

[4]Department of Bioengineering, University of Pennsylvania, Philadelphia, PA

[5]Department of Radiology, University of Pennsylvania, Philadelphia, PA

[6]Department of Congenital Heart Disease, Evelina London Children's Hospital, UK

[7]Division of Cardiology, Children's Hospital of Philadelphia, Philadelphia, PA

[8]Department of Cardiology, Boston Children's Hospital, Boston, MA

Abstract

Background: Repair of complete atrioventricular canal (CAVC) is often complicated by atrioventricular valve regurgitation, particularly of the left-sided valve. Understanding the three-dimensional (3D) structure of the atrioventricular canal annulus prior to repair may help to inform optimized repair. However, the 3D shape and movement of the CAVC annulus has yet to be quantified nor has it been rigorously compared to a normal mitral valve annulus.

Methods: The complete annuli of 43 patients with CAVC were modeled in 4 cardiac phases using transthoracic 3D echocardiograms and custom code. The annular structure was compared to the annuli of 20 normal pediatric mitral valves using 3D metrics and statistical shape analysis (Procrustes analysis).

Results: The unrepaired CAVC annulus varied in shape significantly throughout the cardiac cycle. Procrustes analysis visually demonstrated that the average normalized CAVC annular shape

Corresponding author: Matthew Jolley, Children's Hospital of Philadelphia, 3401 Civic Center Blvd, Philadelphia, PA 19104, jolleym@email.chop.edu.

is more planar than the normal mitral annulus. Quantitatively, the annular height to valve width ratio of the native left CAVC atrioventricular valve was significantly lower than that of a normal mitral valve in all systolic phases($p<0.001$).

Conclusions: The left half of the CAVC annulus is more planar than that of a normal mitral valve with an annular height to valve width ratio similar to dysfunctional mitral valves. Given the known importance of annular shape to mitral valve function, further exploration of the association of 3D structure to valve function in CAVC is warranted.

Keywords

CHD; septal defects; Echocardiography; Mitral Valve

Common atrioventricular canal defect (CAVC) is a developmental abnormality whereby there is one atrioventricular valve (AVV) over both ventricles with a single annulus. In the current era, repair of CAVC is typically performed in the first 6 months of life. Despite low operative mortality, hemodynamically significant atrioventricular valve regurgitation (AVVR) occurs in up to 40% of patients.(1–3) Results of surgical reintervention are poor with more than a quarter of patients requiring two reoperations or more.(4, 5) Previous reports suggest that different surgical techniques are not associated with different surgical outcomes. This observation suggests that underlying structural contributions to AVVR may be incompletely understood.(6)

In adults, the understanding of the dynamic three-dimensional (3D) structure of the mitral valve has progressed significantly with the advancement of 3D echocardiography (3DE).(7, 8) Normal mitral valve annular shape has been demonstrated to be important to valve function(9, 10) and this understanding has informed structurally targeted annuloplasty therapies such as non-planar annuloplasty rings.(11, 12) During CAVC repair, the surgeon divides the common valve into two valves. The resulting atrioventricular annular shape is thus the product of both the native anatomy and the surgical repair. As such, a detailed understanding of the native CAVC annular shape and motion may inform design and application of surgical repair that better replicates the “normal” atrioventricular valves.

In this study, our primary goal was to compare the morphologic features of the unrepaired CAVC valve annulus to normal mitral valves. We also sought to characterize, visualize, and quantify the dynamic shape and motion of the CAVC annulus.

Material and Methods

Subjects

Institutional databases at the Children’s Hospital of Philadelphia (CHOP), Boston Children’s Hospital, and Evelina London were used to retrospectively identify patients with CAVC in whom transthoracic 3DE had been collected for clinical studies between 2016 and 2019. To augment these unsedated studies, dedicated acquisitions in the OR prior to repair were obtained at CHOP between 2016 and 2019. These latter studies were obtained with parental consent per an institutional review board (IRB) approved protocol. For a control group, 3DE of the mitral valves of children without known pathology and otherwise

normal echocardiograms were identified.(13) These children were on average older than the children in the CAVC group, due to the lack of existing availability of or ethical means of obtaining dedicated sedated echocardiograms of normal children in the age 2-6 month range typical of CAVC repair. Exclusion criteria for all studies included presence of significant stitch artifact, lack of inclusion of the entire valve annulus in the acquisition, and inability to delineate the valve annulus. This study was performed according to a protocol approved by the IRB at each site.

Transthoracic Image Acquisition

3DE images were acquired using Full Volume gated acquisitions. Transthoracic X7 or X5 probes were used with the Philips IE33 and EPIQ 7 ultrasound systems (Philips Medical, Andover, MA). Qualitative assessment of ventricular function and degree of AVVR were drawn from clinical reports as there is no accepted quantitative grading scale for AVVR in CAVC. Identification of Rastelli type (Figure S1) was drawn from clinical reports and confirmed by visual inspection of the 2-dimensional and 3D echo images. Postoperative studies were performed prior to discharge from the hospital.

Annular Curve Modeling and Quantification

3DE images of the CAVC and normal mitral patients were imported into the QLAB 10.4 CV 3D module (Philips Medical, Andover, MA), exported as Cartesian Digital Imaging and Communications in Medicine format, and then imported into 3D Slicer (www.slicer.org). (14, 15) CAVC, mitral, and aortic annular curve modeling was performed using 3D Slicer as demonstrated in Figure 1 and as previously described.(14) Aortic annular modeling was included to demonstrate differences in relationships of the aortic annulus to the CAVC valve compared to normal mitral valves. In total, 4 equally spaced cardiac phases were modeled for CAVC. Analysis began with the identification of anatomic landmarks and selection of the end-diastolic (ED) frame (first frame with valve closed) and the end-systolic (ES) frame (last frame before valve opens). The single mid-systolic (MS) frame was defined as the frame midway between these two frames. Similarly, the mid-diastolic (MD) frame was defined as the frame halfway between valve opening and valve closing. Normal mitral valve modeling was also performed in the same phases.

Quantification was performed using Euclidian geometry in custom code using the metrics displayed in Figure 2, as previously described in detail.(14) Annular height was calculated as the distance from the highest point on the annulus to the lowest point on the annulus relative to a least squares plane. Given the visual differences in annular shape we created two analogous metrics to compare the non-planarity of the normal mitral valve to the left side of the CAVC valve (Figure 3). Annular height to valve width ratio (AHWR) was defined as annular height / antero-lateral (AL) to posterior medial (PM) diameter ratio (often described as the annular height to commissural width ratio –AHCWR -- for normal mitral valves). For CAVC we calculated two AHWR metrics: left annular height / LA-LP diameter for the left CAVC annulus and total CAVC annular height / LA-LP diameter. LA-LP distance was chosen as the shortest opposing distance on the left CAVC annulus, analogous to the AL-PM distance in the normal mitral valve. Bending angle for the CAVC annulus was calculated by fitting a least squares plane to the left half the CAVC annulus as

well as the right half of the CAVC annulus and calculating the angle between them. Annular 3D area was calculated by fitting a least area manifold surface (the surface a “soap bubble” would make on the annulus) to the annulus.(8, 14) To further quantify changes in annular shape and motion, the full annular area was divided into quadrants (Figure 2C). Annular metrics were compared between the four modeled phases. In order to compare the length of the left ventricular outflow tract in CAVC and mitral valves, we quantified the distance from the center of the left AVV to the center of the aortic valve (LC-AC distance, Figure 2B). Procrustes analysis -- a type of shape analysis which allows the calculation of a mean shape of a group of individual shapes – was used.(14, 16) This analysis was applied to annular points in order to optimize alignment of translation and rotation of the annular shapes for the 4 different phases of the cardiac cycle across various cohorts, and generate a mean shape for CAVC and mitral groups (Figures S2, S3, S4, S5).

Statistics

Annular area measures were normalized to BSA, and linear measures were normalized to $BSA^{0.5}$, as previously described.(14, 17) Continuous variables are presented as median [IQR]. Friedman’s Test was utilized to compare annular metrics throughout the cardiac cycle. Comparisons of continuous variables between categorical variables were made using Mann-Whitney U-test. Intra-observer and inter-observer agreement for 17 annular measurements, each at 4 different phases of the cardiac cycle, were taken on 15 different 3DE datasets (Table S5) and compared using interclass correlation coefficient (ICC). All analysis was performed using RStudio version 1.1.456 (R Studio, Inc., Boston, MA).

Results

The complete CAVC annuli and aortic annuli were modeled in each of the cardiac phases (ED, MS, ES, and MD) in a total of 43 patients. Thirty-five (81%) of these patients had Trisomy 21. The median age of the CAVC patients at echo was 3 months [IQR 2-4 months]. 25 patients had Rastelli type A, and 18 patients had Rastelli type C anatomy. 41 patients had qualitatively normal ventricular systolic function and 2 patients had mildly diminished ventricular systolic function (Table 1). Normal mitral patients were older and larger than CAVC patients ($p < 0.05$, Table 1).

Dynamic Motion and Shape Change of the CAVC Annulus

The mean shape of the CAVC annulus at each of the four phases throughout the cardiac cycle was determined using Procrustes analysis, as shown in Figures S2 and S4. An animation of a representative annulus moving through 4 cardiac phases is shown in Video 1. The CAVC annular area, diameters, and circumference all changed significantly throughout the cardiac cycle, contracting from ED to ES (Table S1 and S2). The bending angle between the right and left halves of the annulus also varied significantly, flattening by on average 10 degrees from ED to ES. The total annular height, as well as the individual right and left side annular heights, did not vary significantly throughout the cardiac cycle.

On average, all annular quadrants moved symmetrically throughout the cardiac cycle with no clear differences in movement between quadrants (Figure 2C, Table S2). Reproducibility of annular modeling was excellent using ICC as shown in Table S5.

Comparison of CAVC Valve by Subgroup (Rastelli Type)—The mean annular shape in ED, MS, ES, and MD of the Rastelli Type A (n=25) and Rastelli Type C (n=18) patients is shown in Figure S5. Quantitative comparison of annular metrics is shown in Table S4. Overall there were not substantial differences in annular shape between the two subgroups (all $p>0.10$).

Comparison of the CAVC Annulus to the Normal Mitral Valve Annulus

A comparison of the mean shape of the CAVC annulus and the normal mitral valve annulus in mid-systole is shown in Figure 4. The mean shape of the CAVC and mitral valve annuli in all phases are shown in Figures S2, S3, and S4. An animation of the mean shape of the CAVC and mitral valve annulus moving through the cardiac phases is shown in Video 1. Visually the mean shape of the left half of the CAVC annulus appeared to be more planar (smaller annular height to valve width ratio), compared to the mitral valve annulus. Quantitatively the left AHWR was significantly lower in the CAVC ($p<0.001$ in all phases) relative to normal mitral valves as shown in Table 2. Annular height was also significantly lower in patients with CAVC, and the annular width was greater ($p<0.01$ for both, all phases). The distance from the center of the left half of the CAVC valve to the aorta (LC-AC distance, Figure 2B) was significantly greater ($p<0.001$ in all phases) compared to the distance from the center of the mitral valve to the aorta (MC-AC distance) as shown in Table S3.

Comment

We present a detailed analysis of visualization and quantification of the dynamic native CAVC annulus and leaflets using 3DE. We believe this is the first quantitative description of the dynamic annular motion of the native, unrepaired CAVC valve using 3DE. It is also the first quantitative comparison of the structure of native CAVC valve annuli to normal mitral valve annuli.

Our major finding was that the shape of the left CAVC annulus is significantly more planar than the annulus of a normal mitral valve, with an AHWR typical of a dysfunctional mitral valve in the biventricular heart (AHWR<15).

Implications for Valve Dysfunction

The non-planar, saddle shape of the normal mitral annulus (AHWR ~ 25) has been demonstrated in engineering simulations to be important for reducing mitral leaflet and papillary muscle stress.(8) Clinically, a more planar mitral annulus has been associated with degenerative valve disease and mitral regurgitation in both children and adults, manifesting as increased leaflet billow and papillary chordal rupture.(18) As such, maintenance of the normal mitral annular shape is thought to be structurally important; non-planar annuloplasty

rings based on the normal mitral annular shape are commercially available and routinely used during surgical mitral valve repair.(19)

In previous work, Takahashi et al examined the annular structure of the left AVV annulus in patients with CAVC after repair.(20) They demonstrated significant differences in the annular height to left ventricular length ratio between normal mitral controls and the left AVV *after* repair. Further, lower annular height after repair was associated with moderate or greater regurgitation. However, it was unknown whether these findings were due to the *preexisting* structure of the CAVC, or the result of the "composite" annular structure determined both by the native anatomy and the surgical addition. In our study, the median CAVC left AVV AHWR was 14, which is less than the mitral AHWR found in normal children and adults (AHWR ~ 25), and in the range of children and adults with degenerative mitral valve disease or connective tissue disease such as Marfan syndrome.(18, 21) In this context, the relatively planar native CAVC annular structure may contribute to a more planar shape after repair, which may in turn be relevant to the lack of durability of left AVV function after repair of CAVC. However, to our knowledge, there is no published CAVC repair technique the goal of a normal, non-planar mitral annular shape for the left AVV. In the absence of a known intervention targeting creation of a more normal annular shape, it is difficult to directly test the importance of annular planarity to left AVV function after CAVC repair. As such, the importance of annular shape in CAVC can only be inferred by the known importance of annular shape to mitral valve disease in children and adults, and by previous work demonstrating that in CAVC a more planar annular shape is associated with increased AVVR. New repair techniques would need to be developed and applied to directly demonstrate the potential benefit of a more normal mitral annular shape to durable repair of the left AVV. In addition, leaflet and papillary muscle structure are known contributors to the durability of left AVV function after CAVC repair.(1, 20) It is unknown whether creation of the stereotypic mitral annular shape can be achieved while creating optimal support of the CAVC leaflets via the subvalvar apparatus. In other words, it remains to be demonstrated that the optimal annular shape for a mitral valve is the optimal annular shape for the left AVV after repair of CAVC. Future work is needed to design, implement, and validate novel strategies guided by structural optimization in this complex population.(22)

Limitations

Our study is retrospective. Patients with CAVC were younger than the patients in the normal mitral group due to the lack of available mitral 3D images in children with full echocardiograms demonstrating normal anatomy in the age group undergoing CAVC repair. There is not a clear indication for sedation (to enable optimal 3DE acquisition) in normal children in this age group. However, we have shown that the mitral annular shape (and specifically AHWR) to be highly preserved from neonate to young adult, (13) and given the large differences in shape, this age difference is unlikely to influence our conclusions. Despite the clear differences in annular shape and height by visualization of mean annular shape, quantitative comparison of the mitral annulus to the CAVC annulus is challenging due to the lack of a septum in the CAVC annulus; metrics are representative, but not identical. However, the annular width utilized for all quantification in CAVC was the smallest annular diameter (denominator of AHWR) available on the left valve, and

would as such tend to overestimate AHWR, not underestimate AHWR. Analysis was done semi-automatically by experienced modelers which requires training, is time-consuming, and contributes to variability. Our analysis focused on the annulus and did not model leaflets or papillary muscles which are clearly relevant to CAVC valve function.(1, 20)

Conclusions

The left side of the native CAVC annulus is significantly more planar than the normal mitral annulus. Given the known association of loss of the normal mitral shape to valve dysfunction, this structural feature may be relevant to the lack of durable left AVV function in CAVC. Additional studies are needed to further elucidate the relationship of 3D valve structure to valve function in CAVC.

Supplementary Material

Refer to Web version on PubMed Central for supplementary material.

Abbreviations

3D	Three Dimensional
3DE	Three-dimensional Echocardiography
AHWR	Annular Height to Width Ratio
AL	antero-lateral
AVV	Atrioventricular Valve
AVVR	Atrioventricular Valve Regurgitation
CAVC	Complete Atrioventricular Canal
Echo	Echocardiography
ED	End-diastole
ES	End-systole
MR	Mitral Valve Regurgitation
MD	Mid-diastole
MS	Mid-systole
PM	Posterior Medial

References

1. Ho DY, Katcoff H, Griffis HM, Mercer-Rosa L, Fuller SM, Cohen MS. Left valvar morphology is associated with late regurgitation in atrioventricular canal defect. Ann Thorac Surg 2020;110(3):969–978. [PubMed: 32088289]
2. Xie O, Brizard CP, d'Udekem Y et al. Outcomes of repair of complete atrioventricular septal defect in the current era. Eur J Cardiothorac Surg 2014;45(4):610–617. [PubMed: 24057432]

3. St Louis JD, Jodhka U, Jacobs JP et al. Contemporary outcomes of complete atrioventricular septal defect repair: Analysis of the society of thoracic surgeons congenital heart surgery database. J Thorac Cardiovasc Surg 2014;148(6):2526–2531. [PubMed: 25125206]
4. Prifti E, Bonacchi M, Baboci A, Giunti G, Krakulli K, Vanini V. Surgical outcome of reoperation due to left atrioventricular valve regurgitation after previous correction of complete atrioventricular septal defect. J Card Surg 2013;28(6):756–763. [PubMed: 24224745]
5. Stulak JM, Burkhart HM, Dearani JA et al. Reoperations after initial repair of complete atrioventricular septal defect. Ann Thorac Surg 2009;87(6):1872–1877; discussion 1877-1878. [PubMed: 19463612]
6. Kaza E, Marx GR, Kaza AK et al. Changes in left atrioventricular valve geometry after surgical repair of complete atrioventricular canal. J Thorac Cardiovasc Surg 2012;143(5):1117–1124. [PubMed: 22078711]
7. Mahmood F, Matyal R. A quantitative approach to the intraoperative echocardiographic assessment of the mitral valve for repair. Anesth Analg 2015;121(1):34–58. [PubMed: 26086507]
8. Salgo IS, Gorman JH 3rd, Gorman RC et al. Effect of annular shape on leaflet curvature in reducing mitral leaflet stress. Circulation 2002;106(6):711–717. [PubMed: 12163432]
9. Bartels K, Thiele RH, Phillips-Bute B et al. Dynamic indices of mitral valve function using perioperative three-dimensional transesophageal echocardiography. J Cardiothorac Vasc Anesth 2014;28(1):18–24. [PubMed: 24011875]
10. Grewal J, Suri R, Mankad S et al. Mitral annular dynamics in myxomatous valve disease: New insights with real-time 3-dimensional echocardiography. Circulation 2010;121(12):1423–1431. [PubMed: 20231533]
11. Jimenez JH, Liou SW, Padala M et al. A saddle-shaped annulus reduces systolic strain on the central region of the mitral valve anterior leaflet. J Thorac Cardiovasc Surg 2007;134(6):1562–1568. [PubMed: 18023684]
12. Levack MM, Jassar AS, Shang EK et al. Three-dimensional echocardiographic analysis of mitral annular dynamics: Implication for annuloplasty selection. Circulation 2012;126(11 Suppl 1):S183–188. [PubMed: 22965981]
13. Jolley MA, Ghelani SJ, Adar A, Harrild DM. Three-dimensional mitral valve morphology and age-related trends in children and young adults with structurally normal hearts using transthoracic echocardiography. J Am Soc Echocardiogr 2017;30(6):561–571. [PubMed: 28391001]
14. Nguyen AV, Lasso A, Nam HH et al. Dynamic three-dimensional geometry of the tricuspid valve annulus in hypoplastic left heart syndrome with a fontan circulation. J Am Soc Echocardiogr 2019;32(5):655–666 e613. [PubMed: 30826226]
15. Fedorov A, Beichel R, Kalpathy-Cramer J et al. 3d slicer as an image computing platform for the quantitative imaging network. Magn Reson Imaging 2012;30(9):1323–1341. [PubMed: 22770690]
16. Pouch AM, Vergnat M, McGarvey JR et al. Statistical assessment of normal mitral annular geometry using automated three-dimensional echocardiographic analysis. Ann Thorac Surg 2014;97(1):71–77. [PubMed: 24090576]
17. Sluysmans T, Colan SD. Theoretical and empirical derivation of cardiovascular allometric relationships in children. J Appl Physiol (1985) 2005;99(2):445–457. [PubMed: 15557009]
18. Lee AP, Hsiung MC, Salgo IS et al. Quantitative analysis of mitral valve morphology in mitral valve prolapse with real-time 3-dimensional echocardiography: Importance of annular saddle shape in the pathogenesis of mitral regurgitation. Circulation 2013;127(7):832–841. [PubMed: 23266859]
19. Vergnat M, Levack MM, Jassar AS et al. The influence of saddle-shaped annuloplasty on leaflet curvature in patients with ischaemic mitral regurgitation. Eur J Cardiothorac Surg 2012;42(3):493–499. [PubMed: 22351705]
20. Takahashi K, Mackie AS, Thompson R et al. Quantitative real-time three-dimensional echocardiography provides new insight into the mechanisms of mitral valve regurgitation post-repair of atrioventricular septal defect. J Am Soc Echocardiogr 2012;25(11):1231–1244. [PubMed: 23022090]

21. Jolley MA, Hammer PE, Ghelani SJ et al. Three-dimensional mitral valve morphology in children and young adults with marfan syndrome. J Am Soc Echocardiogr 2018;31(11):1168–1177 e1161. [PubMed: 30098871]

22. Sacks M, Drach A, Lee CH et al. On the simulation of mitral valve function in health, disease, and treatment. J Biomech Eng 2019;141(7):0708041–07080422.

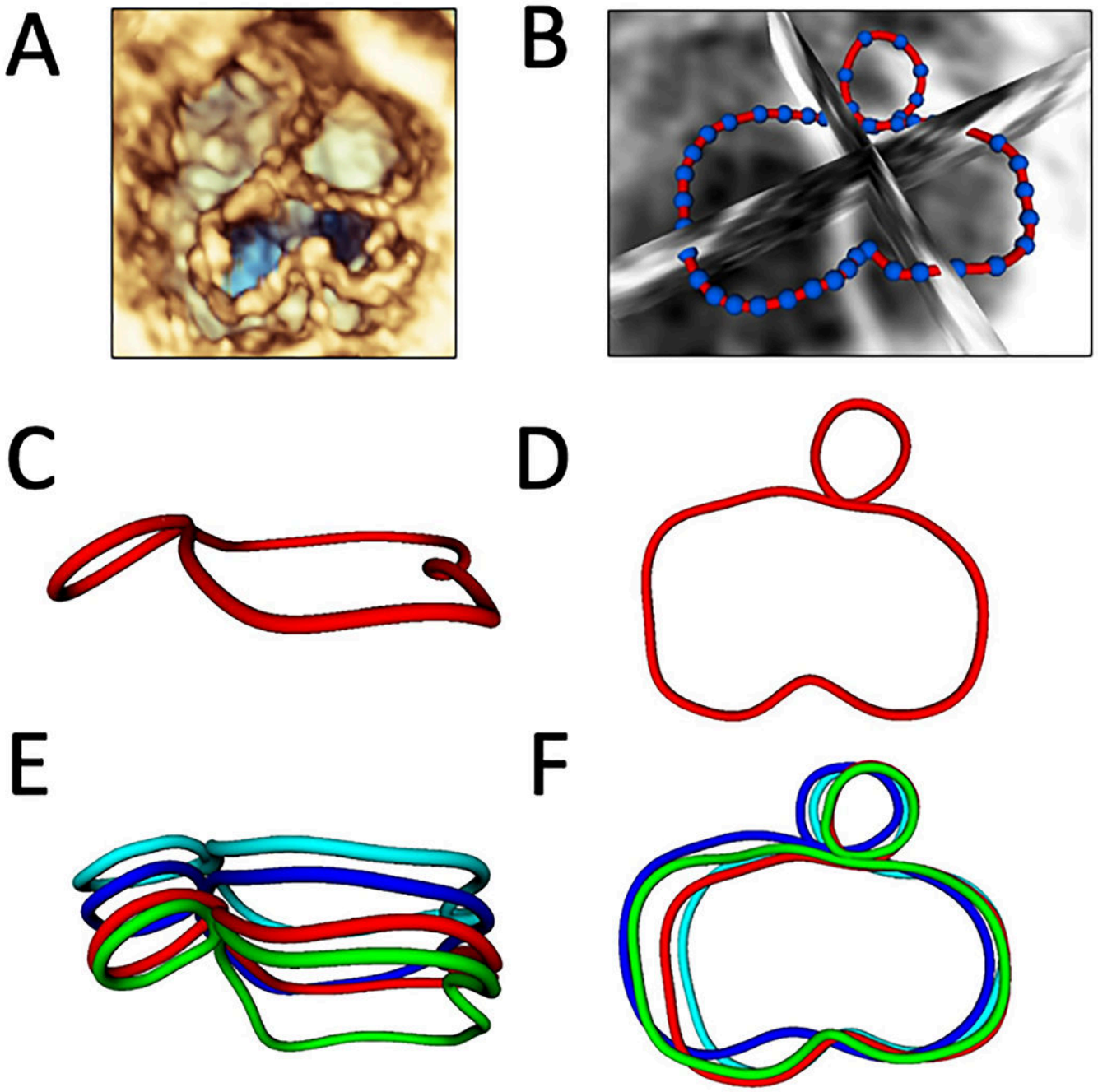

Figure 1. Overview of CAVC Annular Modeling.

A. Volume rendered CAVC annulus from the ventricular view; B. 36 points placed to define valve annulus from the ventricular view; C. Smoothed CAVC and aortic annular contours in mid-systole from a left lateral view; D. Smoothed CAVC and aortic annular contours in mid-systole from the ventricular view; E. CAVC and aortic annular contours in mid-diastole (dark blue), end-diastole (light blue), mid-systole (red), and end-systole (green) from a left lateral view; F. CAVC and aortic annular contours in four phases from the ventricular view.

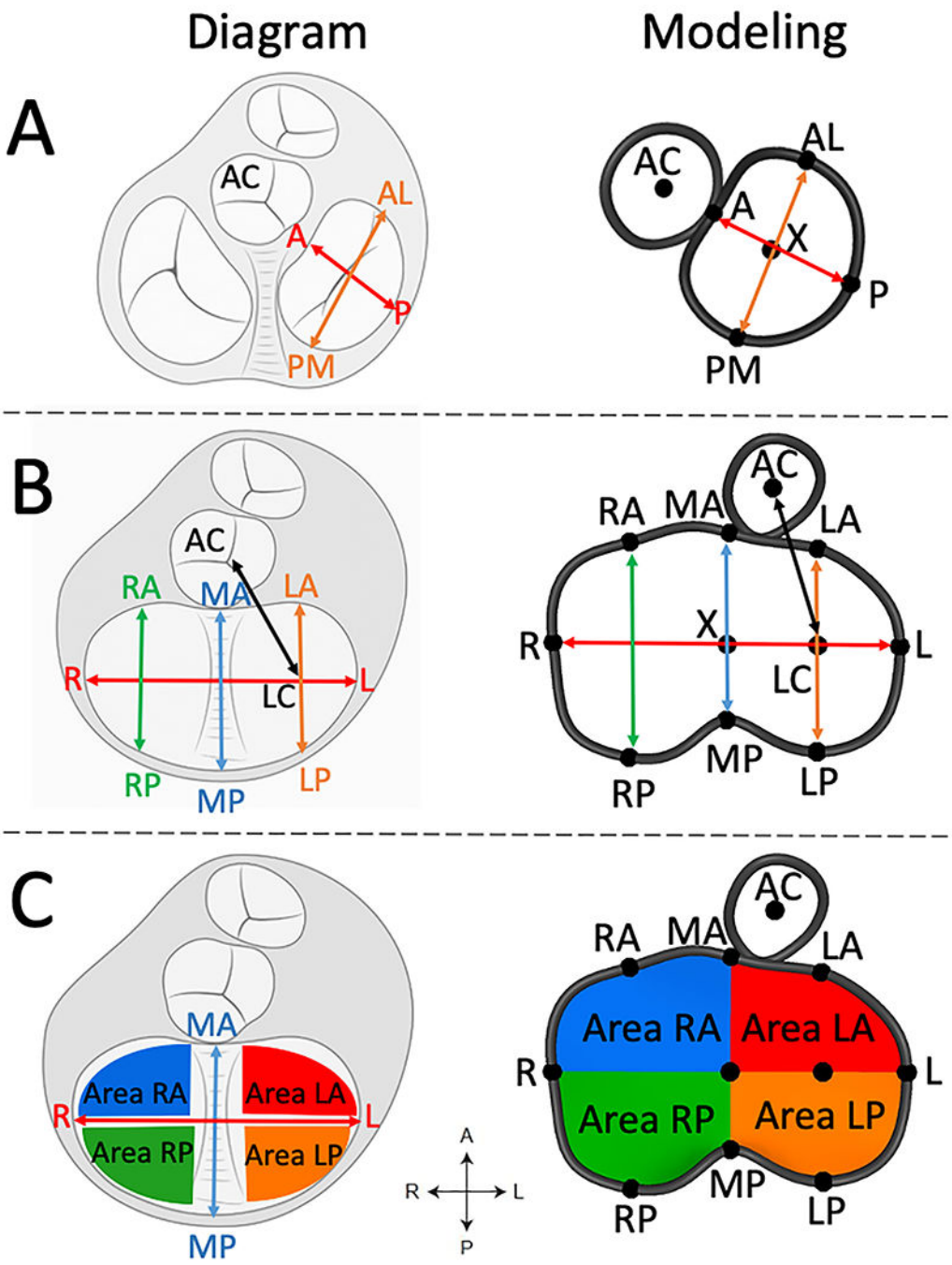

Figure 2. CAVC Annular Measurements from the Ventricular View.

A. CAVC linear annular measurements; B. Division of total CAVC annular area into quadrants. AC = aortic valve centroid, A = anterior, P = posterior, AL = antero-lateral, PM = posterior medial, R = right, L = left, RA = right anterior, MA = mid anterior, LA = left anterior, RP = right posterior, MP = mid posterior, LP = left posterior, LC = left centroid.

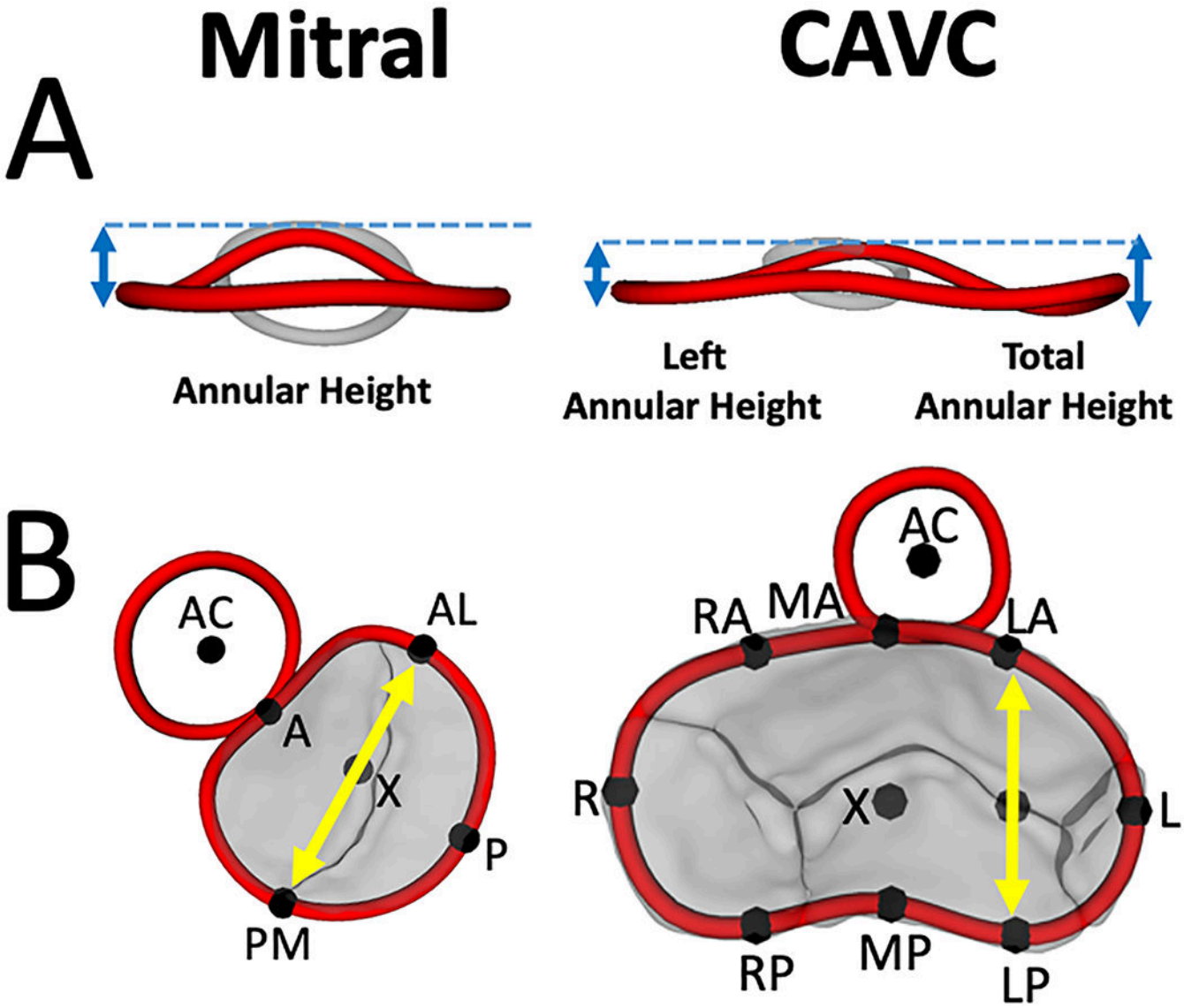

Figure 3. Annular Height and Annular Width Comparisons between Mitral Valve and CAVC in Mid-systole.

A. Annular height comparison between normal mitral valve, left side of CAVC, and total CAVC. B. Annular width comparison between normal mitral valve (AL-PM distance) and CAVC (LA-LP distance). AC = aortic valve centroid, A = anterior, P = posterior, AL = antero-lateral, PM = posterior medial, R = right, L = left, RA = right anterior, MA = mid anterior, LA = left anterior, RP = right posterior, MP = mid posterior, LP = left posterior.

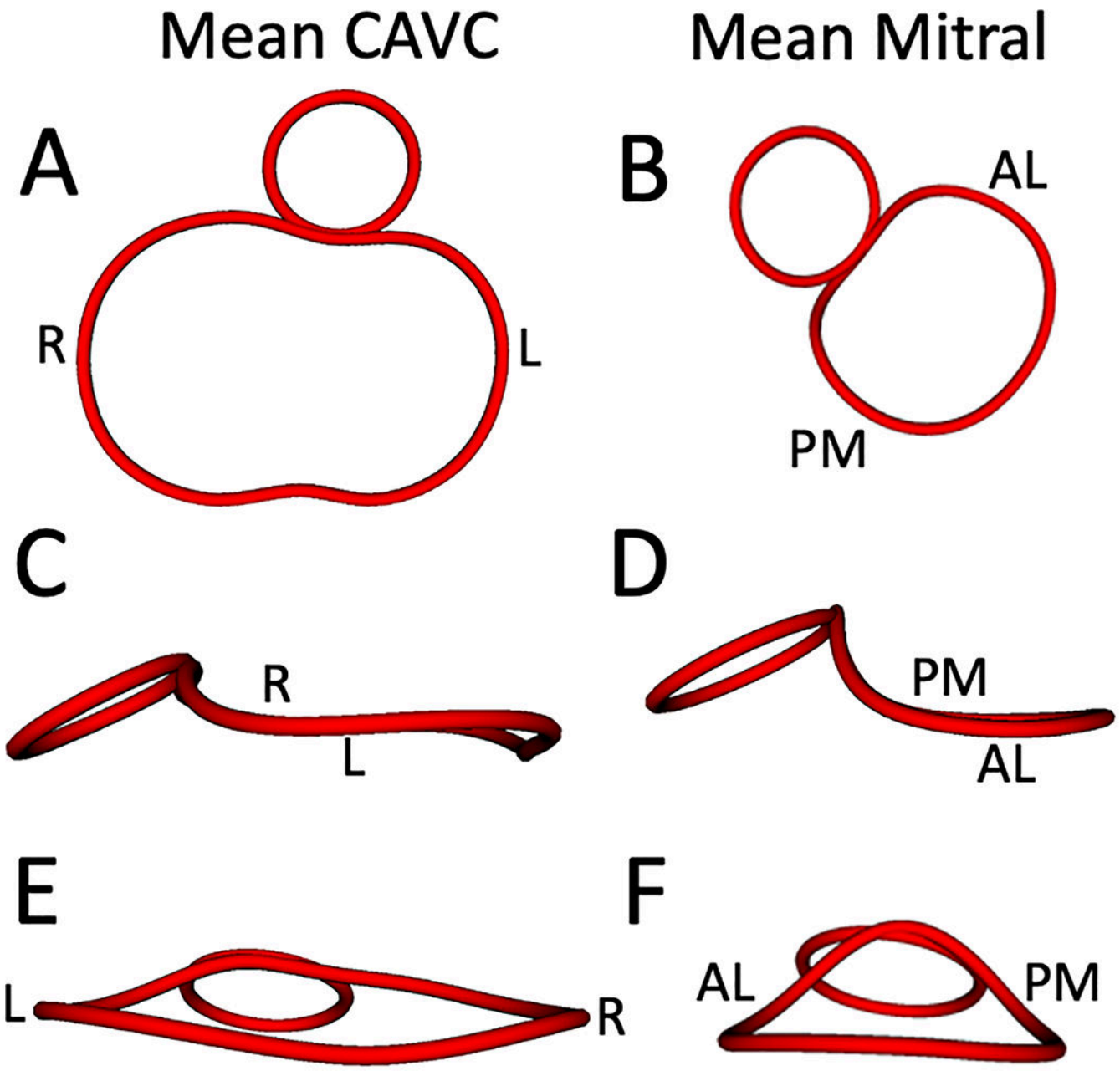

Figure 4. Visualization of Mean CAVC and Mean Mitral Annular Shape in Mid-systole using Procrustes Analysis.

A. Mean CAVC annular shape from the ventricular view; B. Mean mitral annular shape from the ventricular view; C. Mean CAVC annular shape from a left lateral view; D. Mean mitral annular shape from a left lateral view; E. Mean CAVC annular shape from an inferior atrial view; F. Mean mitral annular shape from an inferior atrial view. R = right, L = left, AL = antero-lateral, PM = posterior medial.

Table 1.

Demographics

Variable	CAVC n=43	Normal Mitral n=20
Age (months)	3.0 (2.0-4.0)	30.9 (1.4-38)
Female gender (n, %)	22 (51.2%)	10 (50.0%)
Height (cm)	57 (50, 61)	88 (57, 98)
Weight (kg)	4.5 (3.6, 5.1)	12.9 (4.9, 15.2)
BSA (m^2)	0.27 (0.23, 0.29)	0.57 (0.29, 0.64)
Heart Rate (bpm)	137 (123, 144)	100 (83, 122)
Rastelli Type		
A (n, %)	25 (58%)	
C (n, %)	18 (42%)	
Trisomy 21 (n, %)	35 (81%)	
Qualitative systolic function		
Normal (n, %)	41 (95%)	100%
Mildly diminished (n, %)	2 (4%)	
Moderately diminished (n, %)	0 (0%)	
Pre-Repair AVV Regurgitation		
Mild or less (n, %)	33 (77%)	100%
Moderate or greater (n, %)	10 (23%)	
Post-Repair Left AVV Regurgitation		
Mild or less (n, %)	34 (79%)	
Moderate or greater (n, %)	9 (21%)	
Frame rate (Hz)	34.0 (30.5, 34.0)	30.0 (26.5, 33.0)

BSA = body surface area; AVV = atrioventricular valve.

Data are expressed as median (interquartile range) or as a number (percentage).

Table 2.
Comparison of Annular Metrics of Left CAVC Annuli and Normal Mitral Valves

Variable	CAVC (n=43)	Normal Mitral (n=20)	*p* Value
Left Annulus Height (mm/m)			
End-diastole	4.7 [4.1, 6.0]	6.7 [6.0, 7.2]	<0.001*
Mid-systole	4.8 [3.4, 6.2]	7.3 [6.8, 8.4]	<0.001*
End-systole	4.6 [3.3, 6.1]	6.7 [6.1, 7.7]	<0.001*
Mid-diastole	5.1 [3.7, 5.8]	6.3 [5.8, 7.2]	0.003*
Annulus Width (cm/m)			
End-diastole	3.7 [3.3, 4.0]	2.9 [2.8, 3.3]	<0.001*
Mid-systole	3.6 [3.2, 4.1]	2.9 [2.5, 3.1]	<0.001*
End-systole	3.6 [3.2. 4.0]	2.8 [2.5, 3.0]	<0.001*
Mid-diastole	3.7 [3.4, 4.1]	3.0 [2.7, 3.2]	<0.001*
Left AHWR			
End-diastole	14 [10, 16]	22 [20, 24]	<0.001*
Mid-systole	14 [9, 17]	27 [24, 30]	<0.001*
End-systole	14 [9, 17]	25 [20, 30]	<0.001*
Mid-diastole	13 [9, 17]	21 [20, 23]	<0.001*
Total AHWR			
End-diastole	18 [15, 22]	22 [20, 24]	0.002*
Mid-systole	19 [16, 23]	27 [24, 30]	<0.001*
End-systole	21 [17, 26]	25 [20, 30]	0.050*
Mid-diastole	18 [14, 24]	21 [20, 23]	0.024*

AHWR = annular height to width ratio

Annulus Width: For CAVC = LA-LP Distance; For Normal Mitral = AL-PM distance;

Left AHWR = For CAVC = Left annulus height / LA-LP Distance; For Normal Mitral = Total annulus height / AL-PM distance

Total AHWR = Total annulus height / LA-LP Distance; For Normal Mitral = Total annulus height / AL-PM distance

Values listed are Median [IQR]

* $p<0.05$